Preparation of Regular Micropitted Polylactide Films via Phase Separation and Their Cell Affinity Evaluation

Ye Tian,[1,2] Yingjun Wang,[1,2] Changren Zhou,[3] Qinhui Zeng[3]

[1]*Key Laboratory of Special Functional Materials (Ministry of Education), South China University of Technology, Guangzhou 510641, China*
[2]*School of Materials Science and Engineering, South China University of Technology, Guangzhou 510641, China*
[3]*Department of Materials Science and Engineering, Jinan University, Guangzhou 510632, China*

Received 28 October 2008; accepted 26 June 2009
DOI 10.1002/app.31069
Published online 22 February 2010 in Wiley InterScience (www.interscience.wiley.com).

ABSTRACT: The microscale topography of biomaterial surfaces has a great effect on the adhesion and proliferation behavior of cells. In this study, polylactide (PLA) films with regular micropitted surfaces were prepared by a phase-separation technique. The effect of the surface topography on the wettability and cell affinity was investigated with contact angle measurements and osteoblast incubation, respectively. The results showed that the shape of the pits could be controlled by changes in the film-forming parameters, including the PLA solution concentration, nonsolvent content, temperature, and solvent volatilization speed. These patterned films had significantly enhanced hydrophobicity because of the existence of micropits on the surface, and their hydrophobicity increased with the pit size increasing. Osteoblast spreading was improved on the patterned surface, and so was cell adhesion. However, the proliferation of cells on micropitted surfaces showed no distinction from the proliferation on smooth surfaces, and this indicated that the pit pattern had a great effect on the spreading and adhesion of cells but little on the proliferation of cells. © 2010 Wiley Periodicals, Inc. J Appl Polym Sci 116: 3162–3170, 2010

Key words: adhesion; biomaterials; films; phase separation

INTRODUCTION

Interest in micropatterned polymer surfaces, which possess many remarkable properties and functions because of their surface microstructures, as cell culture substrates is increasing in the field of biomaterials. Because the microsize structures on the material surface play an important role in cell behavior,[1–3] some techniques, such as soft lithography[4,5] and the breath-figure method,[6,7] have been developed to fabricate various micropatterned surfaces. However, the application of these methods is limited because most of them require expensive and delicate equipment or have complex preparation processes.

Phase separation is another important procedure for obtaining a regular micropatterned structure, especially in polymer film preparation. In the traditional phase-separation method, the film is prepared by the spreading of a polymer solution onto a solid surface, and the patterned surface is formed through phase separation induced by solvent volatilization. This is restricted to a few kinds of copolymers, which should be specially designed and synthesized, or occurs only under strict thermodynamic conditions.[8,9] Wang et al.[10] developed a simple and low-cost route for fabricating micropitted and nanopitted polystyrene films by spreading polymer solutions onto a nonsolvent surface (SNS). Unlike the film prepared by the traditional method, the film prepared by the SNS method is formed through the phase separation of a polymer solution induced by both the volatilization of the solvent and the exchange between the solvent and nonsolvent. In comparison with the conventional method, the SNS method could be used in many commercially available polymers, and the surface patterns could be easily controlled by adjustments to the film-forming parameters.

Polylactide (PLA) is used commonly as a scaffold support in bone tissue engineering, mainly because of its good biodegradable, biocompatible, and mechanical properties.[11,12] The PLA homopolymer cannot form regularly patterned films via the traditional phase-separation method because of its low hydrophilicity.[13] If the hydrophilicity of PLA is improved, a patterned film may be obtained. Zhao et al.[14] found that poly(lactic-*co*-glycolic acid) with a 50:50 ratio of

Correspondence to: C. Zhou (tcrz9@jnu.edu.cn).
Contract grant sponsors: National Key Technologies R&D Program; contract grant numbers: 2006BAI16B04 and 2006BAI16B06.
Contract grant sponsor: National Basic Research Program of China; contract grant numbers: 2005CB623902.
Contract grant sponsor: National Science Foundation; contract grant numbers: 50732003, 50830101 and 50803018.
Contract grant sponsor: Natural Science Foundation of Guangdong; contract grant numbers: 4205786.

lactic to glycolic acid [PLGA (50:50)] could form a film with a honeycomb structure, but PLGA (90:10) and PLGA (70:30) could not because of their lower hydrophilicity. Fukuhira et al.[15] successfully prepared a honeycomb-patterned film from a PLA homopolymer using a phospholipid as a surfactant.[15] Adding the surfactant to the hydrophobic polymer solution improved the hydrophilicity of the polymer, and honeycomb-patterned films were probably formed.

In this study, we used the SNS method to prepare a series of PLA films with regular micropits without the addition of any surfactant, and we studied the effects of the processing parameters on the surface topography by changing the conditions of phase separation. The wettability of the resultant patterned PLA films was examined with contact angle measurements. The behavior of cells on the patterned surfaces was further investigated with cell morphology observations, attachment efficiency measurements, and methyl thiazolyl tetrazolium (MTT) assay.

EXPERIMENTAL

Materials

PLA was synthesized by microwave-irradiated ring-opening polymerization according to a literature method,[16] and its molecular weight (weight-average molecular weight = 100,000) was measured by gel permeation chromatography (1515-2414, Waters, USA) with tetrahydrofuran (THF) as the solvent. THF, ethylene glycol (EG), and glycerol (GC) were analytical-grade and were purchased from Sigma (USA).

Fabrication of the micropitted PLA films

Micropitted PLA films were prepared by the SNS method. In this method, about 2 mL of a PLA solution in THF was dropped slowly onto the surface of a nonsolvent of the polymer in a 100-mL beaker. The polymer solution droplet spread onto the surface of the nonsolvent; this solidified within several minutes in air to form a semitransparent film with a micropit-patterned surface. The film was washed thoroughly with distilled water and dried *in vacuo*. Factors including the PLA solution concentration (10, 15, or 20% w/v), nonsolvent content (EG, GC, or their mixture with different volume ratios), temperature (10, 30, or 50°C), and pressure (*in vacuo* or under semiclosed conditions) were chosen to study their effects on the surface patterns of PLA films.

Surface characterization

Surface morphology observation

To determine the surface morphology of films, samples were sputter-coated with a 10-nm gold layer and observed under a scanning electron microscope (XL-30 ESEM, Philips, Eindhoven, Holland). The micropit shape and density were evaluated with Image J software, with which 10 micropits were analyzed per film.

Contact angle measurements

The static contact angle of water was used to evaluate the wettability of PLA films with a contact angle meter (Cam-Plus, Unicyro Co., Wimsheim, Germany) at room temperature. Five points on each sample were measured, and the mean values were calculated.

The surface energy (γ) was determined by measurement of the contact angle (θ) of two kinds of reference liquids (water and diiodomethane) and was calculated with harmonic mean equations:[17]

$$(1+\cos\theta_1)\gamma_1 = 4[\gamma_1^{\,d}\times\gamma_s^{\,d}/(\gamma_1^{\,d}+\gamma_s^{\,d}) + \gamma_1^{\,p}\times\gamma_s^{\,p}/(\gamma_1^{\,p}+\gamma_s^{\,p})] \quad (1)$$

$$(1+\cos\theta_2)\gamma_2 = 4[\gamma_2^{\,d}\times\gamma_s^{\,d}/(\gamma_2^{\,d}+\gamma_s^{\,d}) + \gamma_2^{\,p}\times\gamma_s^{\,p}/(\gamma_2^{\,p}+\gamma_s^{\,p})] \quad (2)$$

where γ^d is the dispersive component; γ^p is the polar component; subscripts 1 and 2 refer to water and diiodomethane, respectively; θ_1 is the contact angle of water; and θ_2 is the contact angle of diiodomethane. For water, $\gamma_1 = 72.8$ mJ/m^2, $\gamma_1^{\,d} = 22.1$ mJ/m^2, and $\gamma_1^{\,p} = 50.7$ mJ/m^2. For diiodomethane, $\gamma_2 = 50.8$ mJ/m^2, $\gamma_2^{\,d} = 44.1$ mJ/m^2, and $\gamma_2^{\,p} = 6.7$ mJ/m^2.

Osteoblast incubation

Observation of the osteoblast morphology

The samples were cut into circular pieces and placed in a 96-well cell culture plate (Costar, USA). A 200-μL cell suspension with about 1×10^4 cells was dropped onto the samples, which were cultured in a CO_2 incubator (Shellab Co., USA) with 5% CO_2 at 37°C. After the culturing time was determined, the samples were taken out and washed gently with phosphate-buffered saline (PBS). Thereafter, the cells were fixed with 2.5% glutaraldehyde in PBS for 1 h at 4°C. After being washed with PBS, the samples were dehydrated sequentially in a graded ethanol series twice (50, 70, 80, 90, 95, and 100%, with 3 min at each concentration each time). The fixed samples were freeze-dried and examined with scanning electron microscopy (SEM).

Osteoblast attachment efficiency measurements

After being incubated for 6 h, the cells on the films were rinsed with PBS to remove the unattached cells and then were digested with trypsin. The number of

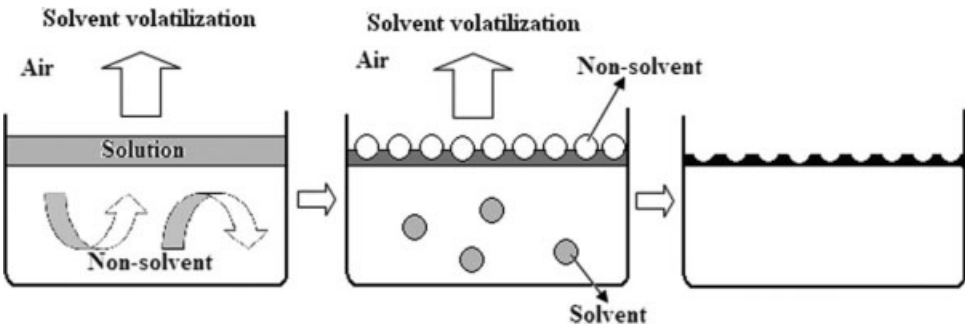

Figure 1 Mechanism of SNS to prepare polymer films with micropits.

cells on the films was counted with a hematocytometer. The cell attachment efficiency was defined as follows:

$$\text{Attachment efficiency}(\%) = \left(\frac{\text{Number of cells on the film}}{\text{Number of planted cells}}\right) \times 100\% \quad (3)$$

Osteoblast proliferation

The proliferation of cells was measured by MTT assay. In brief, a 20-μL MTT solution (5 mg/mL), which was confected with PBS buffer, was placed into each well, and the cells were cultured for 4 h. Then, 150 μL of dimethyl sulfoxide was added after the MTT solution was removed. After 10 min of shaking at 37°C, the absorbency of each well was measured with a microplate reader (MK3, Thermo, USA) at 492 nm. The growth curve was obtained with the time taken as the abscissa and the absorbency taken as the ordinate.

RESULTS AND DISCUSSION

Micropitted-film-formation parameters

Nishida and Shimomura[18,19] reported that a honeycomb structure is formed by the condensation of water droplets from a humid atmosphere on a solution surface in the conventional phase-separation method. In the SNS method, Wang et al.[10] concluded that the nonsolvent of the polymer is the cause of the pattern formation but not the water droplet because they found that similar structures could be obtained under a dry atmosphere and under ambient conditions. Three essential elements, including the polymer, the solvent of the polymer, and the nonsolvent of the polymer, are necessary in the SNS method. Also, it is important for the solvent and

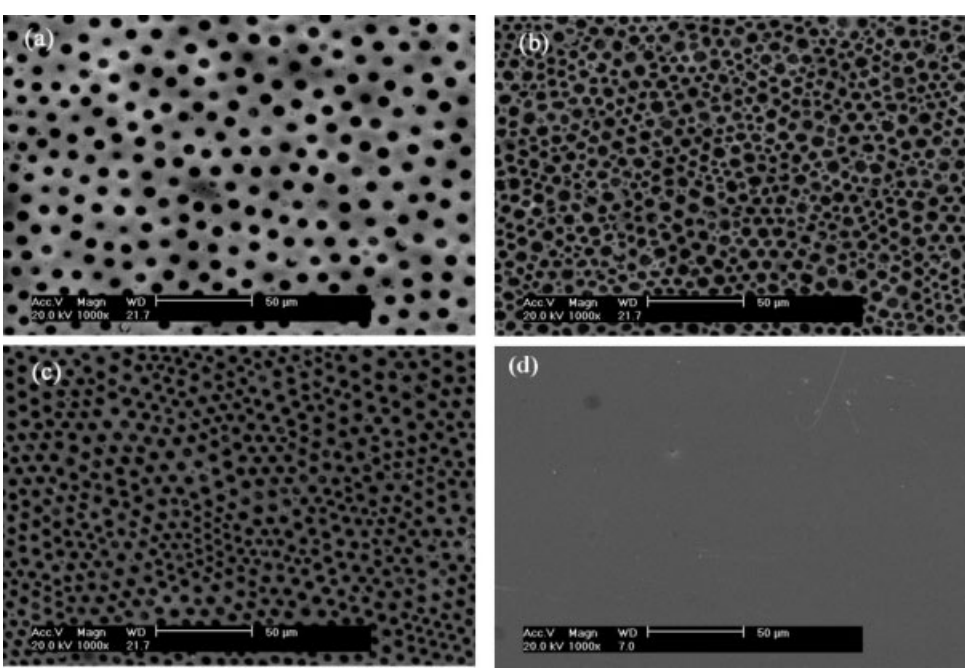

Figure 2 SEM images of surface patterns prepared from the volatilization of PLA solutions at 30°C on GC with different concentrations: (a) 10, (b) 15, and (c) 20% (w/v) and (d) the reverse surface of the film.

TABLE I
Effect of the Solution Concentration on the Structure of the Micropits

Concentration (%)	Diameter (μm)	Density (features/mm^2)	Circularity
10	5.5 ± 0.4	0.9×10^4	0.897
15	3.4 ± 0.2	1.0×10^4	0.886
20	3.0 ± 0.3	2.0×10^4	0.868

nonsolvent to be miscible with each other. In brief, the process of micropit formation might be described as follows (see Fig. 1):

1. When the polymer solution is spread onto the surface of the nonsolvent, the intersolubility between the solvent and nonsolvent causes diffusion of the nonsolvent into the solution.
2. A thin, dense skin is first formed on the interface of the nonsolvent and solution because of the matter exchange, which restricts the diffusion further.
3. The nonsolvent that has diffused in the solution is separated to form a number of microdroplets after volatilization of the solvent.
4. The microdroplet-occupied position is polymer-poor, and the other area is polymer-rich; this causes circular or nearly circular micropit formation on the upper surface of the PLA film, and the shape of the pits is determined by the form of the nonsolvent droplet.

The effects of the film-forming parameters, including the polymer solution concentration, nonsolvent content, temperature, and pressure, on the shape and density of the micropits in the SNS method were studied, and they are discussed next.

Effect of the PLA solution concentration

The shapes and densities of micropits formed with different polymer concentrations are shown in Figure 2 and compared in Table I. PLA films with regular (circularity > 0.85) micropit-patterned surfaces were achieved with solutions of different concentrations. The patterns were formed only on the surface in contact with air, and the surface in contact with the nonsolvent was smooth [Fig. 2(d)]. The pit diameters decreased and the densities increased with the solution concentration increasing. A change in the solution concentration could influence the properties of the polymer solution, such as the viscosity and fluidity. The smaller size and higher density of the pits could be attributed to the high viscosity and low fluidity of the concentrated solution. The quantity of the nonsolvent that diffused into the concentrated solution was less than that of the nonsolvent that diffused into the dilute solution. Furthermore, the high viscosity of the concentrated solution limited the ability of the nonsolvent dissolved in the polymer solution to aggregate, so smaller nuclei were formed with the solvent volatilizing. Therefore, the liquid droplets distributed on the surface of the

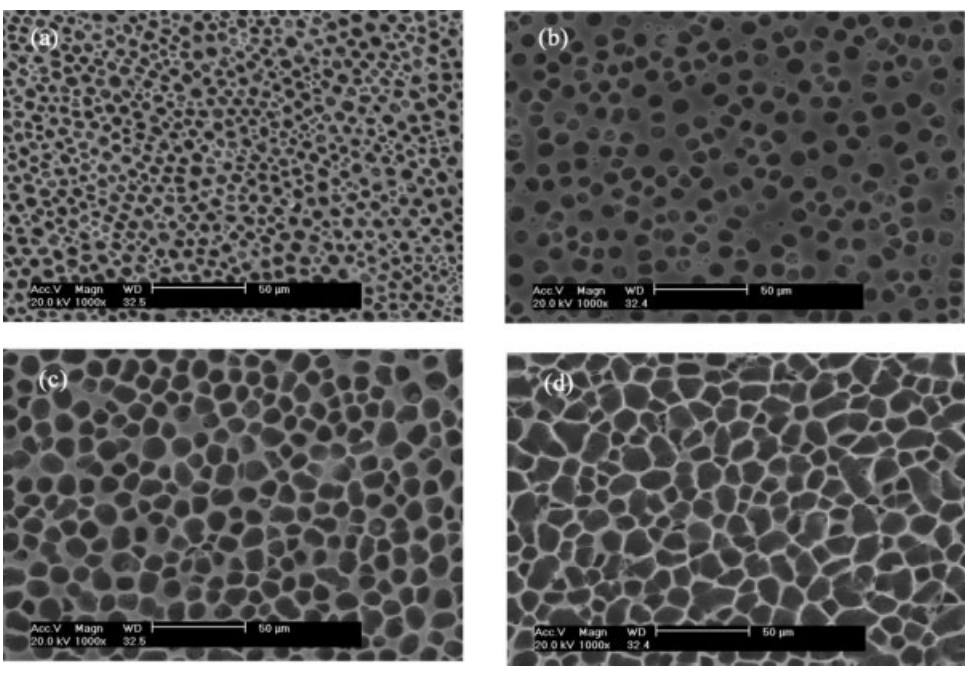

Figure 3 SEM images of surface patterns prepared from the volatilization of a 15% (w/v) PLA solution at 30°C on different nonsolvents: (a) 25% (v/v) EG in GC, (b) 50%;(v/v) EG in GC, (c) 75% (v/v) EG in GC, and (d) 100% EG.

TABLE II
Effect of the Nonsolvent Content on the Structure of the Micropits

Nonsolvent	Diameter (μm)	Density (features/mm^2)	Circularity
25% EG in GC	3.7 ± 0.8	3.0×10^4	0.868
50% EG in GC	4.3 ± 1.2	2.0×10^4	0.860
75% EG in GC	10.3 ± 1.8	1.0×10^4	0.824
EG	17.8 ± 5.2	0.6×10^4	0.787

solidified film from the concentrated solution were smaller and denser than those from the dilute solution. Accordingly, PLA films with pit-patterned surfaces of smaller sizes and higher densities could be formed from the more concentrated solution.

Effect of the nonsolvent content

EG, GC, and their mixtures were selected as nonsolvents to fabricate micropitted PLA films because of their strong polarity and excellent solubility in THF. The nonsolvents had a great influence on the pit shape, as shown in Figure 3 and Table II. Figure 2(b) demonstrates that dense and regular circular micropits could be formed on the surface of PLA films with GC as the nonsolvent. With the fraction of EG in the nonsolvent increasing from 25 to 75%, the size of the micropits increased from 3.727 to 10.284 μm, and the shapes became more random (from 0.868 to 0.824). When pure EG was used as the nonsolvent instead of GC, the diameter of the micropits increased to about 20 μm, which was nearly 5 times greater than the size of micropits formed on the surface of GC; however, the size distribution was wide, and the shape of the pits became very irregular (circularity = 0.787) with thin walls.

In comparison with GC, EG had a lower viscosity and stronger affinity to THF, which caused faster diffusion into the solvent. Large amounts of EG diffused into THF and thus placed the solution in a thermodynamically unstable state, which caused violent phase separation and solution solidification within 1 min. At the same time, masses of EG also gathered easily on the PLA solution surface and formed a number of bigger and irregular microdroplets because of its lower viscosity. (In contrast to EG, the higher viscosity and weaker affinity of GC led to a number of smaller and more regular microdroplets forming on the surface, which induced the patterned surface with the formation of regular micropits.) The results showed that an ideal nonsolvent should possess a high density to support the solution, proper solubility with the solvent, and a high viscosity to form regular microdroplets.

Effect of the temperature

The effect of the environmental temperature on the surface pattern was also studied, as shown in Figure 4 and Table III. When the temperature increased, the size of the micropits decreased. However, the density of the micropits that formed at a lower temperature (10°C) and at a higher temperature (50°C) was lower than the density of micropits formed at room temperature [30°C; see Fig. 2(b)].

A higher temperature led to a smaller pit size and a lower density, and this may be explained by the viscosity and the volatilization of the solvent. Although the viscosities of the nonsolvent and solution were both lower at a higher temperature, it seemed that more GC diffused into the solution to form bigger pits. However, the high temperature also accelerated the volatilization of the solvent, causing film solidification very quickly (within a few minutes). The nonsolvent did not have enough time to diffuse into the solution and aggregate to form bigger droplets; hence, the pits that formed at a higher temperature were poorer and smaller than those formed at room temperature. In contrast to a higher temperature, a lower temperature slowed the solvent volatilization speed, and the film solidified over 0.5 h. Although the higher viscosity decreased the speed of the nonsolvent diffusing into the solution, the nonsolvent still had enough time to form bigger but lower density droplets. Therefore, besides the native properties of the solution and solvent, the

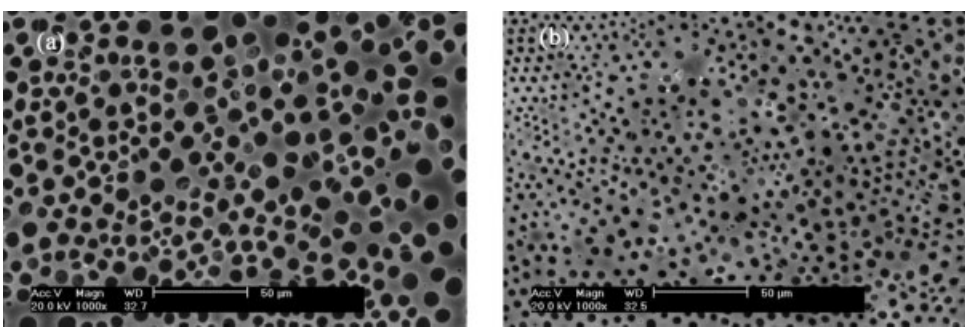

Figure 4 SEM images of the surface patterns prepared from the volatilization of a 15% (w/v) PLA solution on GC at different temperatures: (a) 10 and (b) 50°C.

TABLE III
Effect of the Temperature on the Structure of the Micropits

Temperature (°C)	Diameter (μm)	Density (features/mm^2)	Circularity
10	6.9 ± 0.3	1.4×10^4	0.912
50	3.2 ± 0.6	1.6×10^4	0.838

speed of solvent volatilization also played an important role in patterning the micropits.

Effect of the pressure

To study the effect of pressure on the micropit shape, a beaker with the nonsolvent was put under vacuum conditions or semiclosed conditions to control the surrounding pressure. The diameter of the micropits that formed under the semiclosed conditions (ca. 27 μm) was much bigger than the diameter of the micropits that formed *in vacuo* (ca. 1 μm), and both types of micropits had high densities, as shown in Figure 5 and Table IV. The effect of the surrounding pressure on the surface pattern can mainly be attributed to the volatilization speed. The solvent volatilization speed was much quicker *in vacuo* than under semiclosed conditions. A slow volatilization speed might have allowed GC enough time to diffuse and aggregate to form bigger micropits in comparison with a fast volatilization speed. Furthermore, the micropits fabricated under these two conditions had regular round shapes because they were formed on GC. Controlling the pressure might be an effective way to achieve PLA films with patterned surfaces with regular micropits of the required size.

Wettability and surface energy of the PLA films

As important surface characteristics of biomaterials, wettability and surface energy have great effects on cell adhesion and proliferation.[20,21] Much research has demonstrated that they are determined by the chemical composition and physical morphology of a substance's surface.[22,23] Contact angle measurement is a simple way to evaluate these properties of a sample surface.

TABLE IV
Effect of the Pressure on the Structure of the Micropits

Condition	Diameter (μm)	Density (features/mm^2)	Circularity
Vacuum	1.6 ± 0.2	13.6×10^4	0.905
Semiclosed	27.6 ± 1.8	0.12×10^4	0.867

The water contact angles and surface energies of patterned PLA films with approximately 27- and 1-μm micropits are shown in Table V, with a smooth PLA film surface used as a control. The PLA film with a smooth surface had only moderate hydrophobicity with a water contact angle of 78°. The hydrophobicity of the micropatterned surface showed a significant enhancement. In particular, the contact angle of the patterned surface with approximately 27-μm micropits exceeded 100°. However, it was only 96° on the patterned surface with approximately 1-μm pits, and this showed that the great effect on the hydrophobicity was due to the surface pattern. For the film with bigger micropits, it provided less polymer substrate and more air gaps to support the water droplet; therefore, it had a more hydrophobic surface in comparison with the film with smaller micropits. On the contrary, the surface energy decreased from 24.5 to 17.1 mJ/m^2 with the increase in the pit diameter. These results indicated that the hydrophobicity and surface energy of films could be controlled by changes in the sizes of the pits.

Investigation of the cell affinity

Morphology of the osteoblasts

Osteoblasts are sensitive to the surface morphology of biomaterials. In this research, osteoblasts were selected as model cells to study the effects of the micropitted surfaces of PLA films on cell attachment and growth behavior. The morphologies of cells cultured for 1 or 9 days were observed by SEM, as shown in Figure 6. The height of cells on the smooth

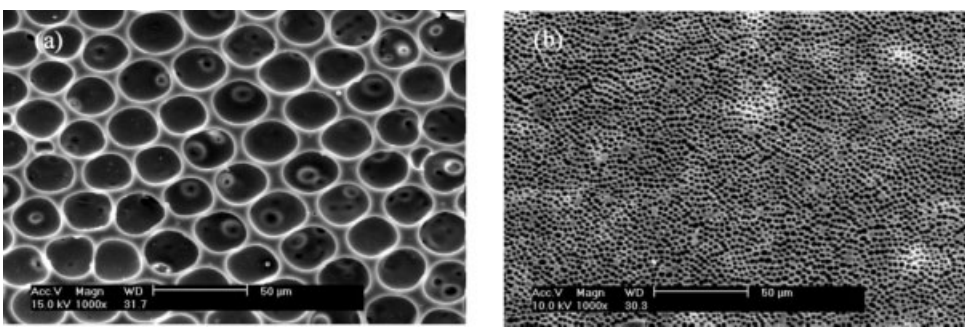

Figure 5 SEM images of the surface patterns prepared from the volatilization of a 15% (w/v) PLA solution on GC in (a) a semiclosed condition and (b) a vacuum condition.

TABLE V
Effects of the Physical Patterns on the Contact Angle and the Surface Energy

Group	$\theta_{(H_2O)}$ (°)	$\theta_{(CH_2I_2)}$ (°)	γ_s (mJ/m^2)	γ_s^p (mJ/m^2)	γ_s^d (mJ/m^2)	X_P
Smooth surface	78	44	42.7	14.1	28.6	0.33
1-μm micropitted surface	96	76	24.5	7.5	17.0	0.31
27-μm micropitted surface	104	102	17.1	10.2	6.9	0.60

X_P is the ratio of the polar component in free energy.

surface [Fig. 6(a)] was higher than that of cells on the micropitted surface [Fig. 6(b,c)] after culturing for 1 day, and this proved that the cells preferred to stretch on the micropatterned surface instead of the smooth surface. The micropits served as anchoring points for the filopodia of cells, which snatched them and thus spread their bodies. Although able to grow along the wall, the cells always strode over and would not grow along the curvature of the wall to intrude inside the 1- or 27-μm-diameter pits in this study. After 9 days of culturing, the surfaces of the smooth and micropatterned films were almost covered with the spreading cells, and few cells could be found inside the pits. The 1-μm micropits, which were much smaller than the cells, could not offer enough room for the cells to grow. However, the cells could not grow in the 27-μm micropits either, which were as big as the cells. Two facts might be used to explain the phenomenon: first, the rigidity of the osteoblast would restrain its body from curving to adhere to the curvature of the wall of the pit, and second, the hydrophobicity of PLA would make the cell prefer to spread over the pit to minimize the area of contact with the PLA surface. Berry et al.[24] made a different observation: fibroblasts grew and large adhesion complexes formed inside 25-μm pits

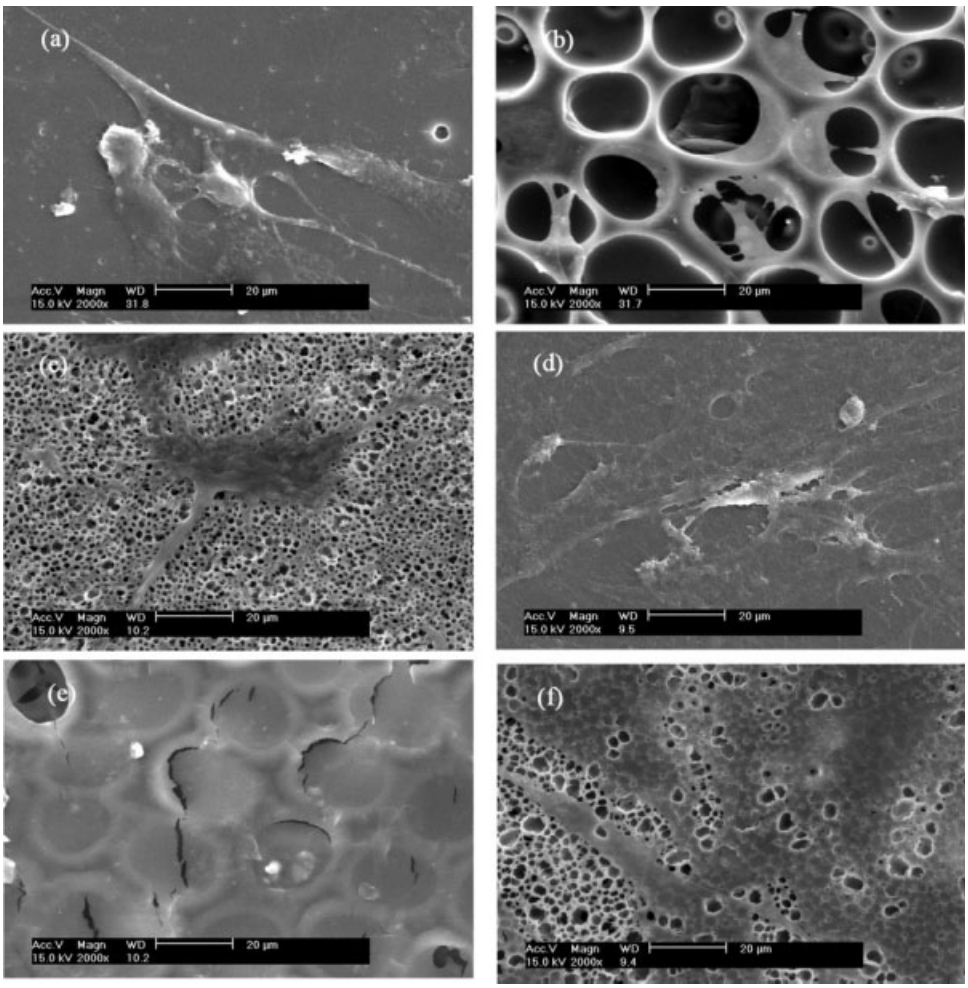

Figure 6 SEM images of osteoblasts cultured for 1 day on PLA films with (a) a smooth surface, (b) a 27-μm micropitted surface, and (c) a 1-μm micropitted surface and 9 days on PLA films with (d) a smooth surface, (e) a 27-μm micropitted surface, and (f) a 1-μm micropitted surface.

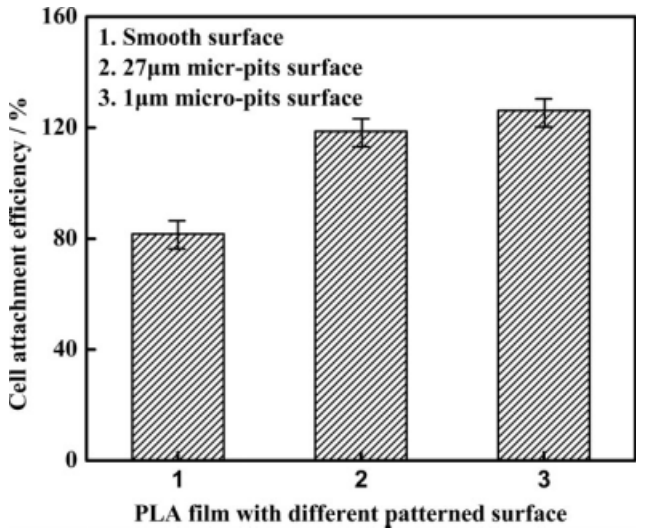

Figure 7 Adhesion efficiency of the osteoblasts on the smooth and micropatterned PLA films.

when quartz was used as the substrate. These different effects might be attributed to the different material surfaces (PLA and quartz, respectively) and various types of cells (osteoblasts and fibroblasts, respectively).[25] The cell morphology on the smooth or pit-patterned surfaces showed specific features that might influence the cell adhesion force on the surfaces.

Adhesion behavior of the osteoblasts

Cell adhesion is a pivotal step influencing cell growth, proliferation, and biofunction. The adhesion efficiencies of cells on smooth and micropitted films are compared in Figure 7. The micropatterned surfaces offered better substrates than smooth surfaces for cell adhesion, although the hydrophobicity was enhanced. Moreover, the cell adhesion efficiency on the 1-μm-pit-patterned surface was higher than that on the 27-μm-pit-patterned surface. The effect of rough surfaces in enhancing cell adhesion might be due to the triggering of subconfluent cells to secrete extracellular proteins allowing the cells to anchor better on their substratum.[23] Furthermore, the surface with 1-μm pits could provide more contact area for the cell filopodia to root than the surface with 27-μm pits. The same phenomenon was observed by Campbell and von Recum.[26] They observed that the size of 1–2-μm pits was beneficial for fibroblast adhesion, and the size of the pits had a greater effect than the hydrophobicity/hydrophilicity of the surface on cell affinity.

Proliferation behavior of the osteoblasts

MTT assay is an indirect method for evaluating cell growth and proliferation. It is based on the theory that only functional mitochondria in living cells can be oxidized by the MTT solution, typically producing a blue-violet end product. The A_{492} value of the end product is correlated to the cell number. The growth curves of osteoblasts on different PLA films were determined by MTT assay to evaluate the cell proliferation behavior, as shown in Figure 8. During the first day, more cells attached to the micropatterned films, and this meant that an improvement of cell attachment had been achieved. After 5 days of culturing, the growth speeds of the cells on all PLA films slowed gradually. From the whole growth curves, it was noted that the cells grew more gently on the PLA film with a micropitted surface than those on the smooth film, although they had better adhesion on the patterned surface. The results indicated that cell proliferation on the micropit-patterned surface showed no distinct improvement in comparison with the control smooth surface. Some similar conclusions were reported when osteoblasts were used as model cells. Kieswetter et al.[27] found that the roughness of a titanium surface could modulate the product of cytokines and growth factors of cells but reduced cell numbers. Wan et al.[28] also indicated that cell proliferation on pit- or island-patterned samples showed no distinct difference in comparison with a control smooth surface, although the cell adhesion was partly improved. Den Braber et al.[29] believed that the influence of micropatterned surfaces on cellular behavior might be caused by the formation of cell–cell contacts. They suggested that the secreted extracellular protein was an initial response of cells to certain micropatterned surfaces that was gradually lost after prolonged incubation. A concrete mechanism is still not clear at the present time.

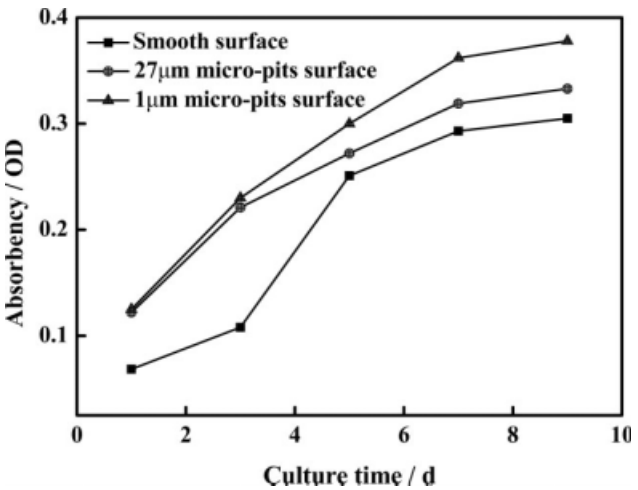

Figure 8 Growth curve of the osteoblasts on the smooth and micropatterned PLA films.

CONCLUSIONS

In this study, thin PLA films with regular micropit-patterned surfaces were fabricated by the SNS method. The exchange between the solvent and nonsolvent and the solvent volatilization were the drivers that induced the formation of pits. They could be adjusted by changes in the film-formation parameters, including the solution concentration, nonsolvent content, temperature, and pressure, to control the size and density of the pits. Osteoblast culturing was performed to evaluate the cell affinity of the PLA films with pit-patterned surfaces. The preliminary results suggested that the patterned surface of a PLA film offered a favorable substrate for cell spreading and adhesion. In comparison with a smooth film, the cells showed better spreading on the patterned surface because these micropits could serve as anchoring points for the filopodia of cells, which snatched them and thus spread their bodies. The adhesion strength of cells was also enhanced on patterned films and especially on the film with 1-μm pits because of the microscale roughness. However, there was no evidence that this surface morphology had an advanced effect on the proliferation of cells. We imagine that a further treatment such as surface modification will be necessary in a future study to improve the cell proliferation behavior on this structure surface.

References

1. Liao, H. H.; Andersson, A. S.; Sutherland, D.; Petronis, S.; Kasemo, B.; Thomsen, P. Biomaterials 2003, 24, 649.
2. Tan, J.; Saltzman, W. M. Biomaterials 2002, 23, 3215.
3. Dalby, M. J.; Giannaras, D.; Richle, M. O.; Gadegaard, N.; Affrossman, S.; Curtis, A. S. G. Biomaterials 2004, 25, 77.
4. Vozzi, G.; Flaim, C.; Ahluwalia, A.; Bhatia, S. Biomaterials 2003, 24, 2533.
5. Lee, C. J.; Blumenkranz, M. S.; Fishman, H. A.; Bent, S. F. B. Langmuir 2004, 20, 4155.
6. Stenzel, M. H.; Barner-Kowollik, C.; Davis, T. P. J Polym Sci Part A: Polym Chem 2006, 44, 2363.
7. Zhao, B. H.; Li, C. X.; Lu, Y.; Wang, X. D.; Liu, Z. L.; Zhang, J. Polymer 2005, 46, 9508.
8. Zhu, H. G.; Ji, J.; Tan, Q. G.; Barbosa, M. A.; Shen, J. C. Biomacromolecules 2003, 4, 378.
9. Otsuka, H.; Nagasaki, Y.; Kataoka, K. Curr Opin Colloid Interface Sci 2001, 6, 3.
10. Wang, Y.; Liu, Z. M.; Han, B. X.; Sun, Z. Y.; Zhang, J. L.; Sun, D. H. Adv Funct Mater 2005, 15, 655.
11. Gong, Y. H.; Zhou, Q. L.; Gao, C.; Shen, J. C. Acta Biomater 2007, 3, 531.
12. Chen, V. J.; Ma, P. X. Biomaterials 2006, 27, 3708.
13. Tian, Y.; Ding, H. Y.; Shi, Y. Q.; Jiao, Q. Z.; Wang, X. L. J Appl Polym Sci 2006, 100, 1013.
14. Zhao, X. Y.; Cai, Q.; Shi, G. X.; Shi, Y. Q.; Chen, G. W. J Appl Polym Sci 2003, 90, 1846.
15. Fukuhira, Y.; Kitazono, E.; Hayashi, T.; Kaneko, H.; Tanaka, M.; Shimomura, M.; Sumi, Y. Biomaterials 2006, 27, 1797.
16. Shu, J.; Wang, P.; Zheng, T.; Zhao, B. X. J Appl Polym Sci 2006, 100, 2244.
17. Yang, J.; Bei, J. Z.; Wang, S. G. Polym Adv Technol 2002, 13, 220.
18. Nishida, J.; Nishikawa, K.; Nishimura, S. I.; Wada, S.; Karino, T.; Nishikawa, T.; Ijiro, K.; Shimomura, M. Polym Sci 2002, 34, 1581.
19. Shimomura, M.; Sawadaishi, T. Curr Opin Colloid Interface Sci 2001, 6, 11.
20. Lee, J. H.; Lee, S. K.; Khang, G.; Lee, H. B. J Colloid Interface Sci 2000, 230, 869.
21. Dahm, M.; Chang, B. J.; Pruker, O. Ann Thorac Surg 2001, 71, 437.
22. Huang, N.; Yang, P.; Leng, Y. X.; Wang, J.; Sun, H.; Chen, J. Y.; Wan, G. J. Surf Coat Technol 2004, 186, 218.
23. Lampin, M.; Warocquier-Clérout, R.; Legris, C.; Degrange, M.; Sigot-Luizard, M. F. J Biomed Mater Res: Part A 1998, 36, 99.
24. Berry, C. C.; Campbell, G.; Spadiccino, A.; Robertson, M.; Curtis, A. S. G. Biomaterials 2004, 25, 5781.
25. Chung, T. W.; Liu, D. Z.; Wang, S. Y.; Wang, S. S. Biomaterials 2003, 24, 4655.
26. Campbell, C. E.; von Recum, A. F. J Invest Surg 1989, 2, 51.
27. Kieswetter, K.; Schwartz, Z.; Hummert, T. W.; Cocharn, D. L.,Simposon, J.; Dean, D. D.; Boyan, B. D. J Biomed Mater Res 1996, 32, 55.
28. Wan, Y. Q.; Wang, Y.; Liu, Z. M.; Qu, X.; Han, B. X. Biomaterials 2005, 26, 4453.
29. den Brader, E. T.; de Ruijter, J. E.; Simts, H. T. J.; Ginsel, L. A.; von Recum, A. F.; Jansen, J. A. Biomaterials 1996, 17, 1093.